Tin-Coupled Star-Shaped Block Copolymer of Styrene and Butadiene (II) Properties and Application

Huadong Feng, Xingying Zhang, Suhe Zhao

Key Laboratory on Preparation and Processing of Novel Polymer Materials, Beijing University of Chemical Technology, Beijing 100029, China

Received 31 January 2008; accepted 19 June 2008
DOI 10.1002/app.28867
Published online 10 October 2008 in Wiley InterScience (www.interscience.wiley.com).

ABSTRACT: A novel tin-coupled star-shaped block copolymer (SB-B)$_4$Sn was synthesized by anionic polymeric techniques. This new copolymer exhibited two different types: One was star-shaped polybutadiene-*b*-poly (butadiene-*ran*-styrene) (*S*-PB-PSB), and the other was star-shaped polybutadiene-*b*-poly(butadiene-*ran*-styrene)-*b*-polystyrene (*S*-PB-PSB-PS). In this article, properties of (SB-B)$_4$Sn were contrasted with that of tin-coupled star-shaped random styrene-butadiene rubber (*S*-SBR) and *S*-SBR/*cis*-BR blend rubbers. Physical property testing results showed that (SB-B)$_4$Sn possessed good mechanical properties like *S*-SBR. Rheological study indicated that these star-shaped block copolymers had good processing properties. Rubber processing analyzer (RPA) spectra showed that the dispersion of additives in (SB-B)$_4$Sn and *S*-SBR/*cis*-BR blend rubber was much better than that in *S*-SBR. Dynamic mechanical thermal analyzer (DMTA) spectra showed that (SB-B)$_4$Sn had a good combination of low rolling resistance and high wet skid resistance, which made it satisfactory materials to produce high performance tire tread.
 J Appl Polym Sci 111: 602–611, 2009

Key words: rubber; mechanical properties; block copolymers; star polymers; morphology

INTRODUCTION

Nowadays, environment concerns and fuel expenses are important to motorists. It has been reported that the energy loss in the tire tread accounted for 30 to 40% of the total loss exhausted by tire.[1,2] So, improved fuel efficiency can be attained by designing tire tread with less rolling resistance. Commonly, rubbers with a high rebound have been considered to containing low rolling resistance property, for example, butadiene rubbers (BR). In addition, rubbers with a coupled structure also have been recognized to have low rolling resistance because these structures contain less free chain terminals.

To motorists, the most important thing is the security. The security of tire is attributed to the traction characteristics on both dry and wet surfaces. To increase the wet skid resistance of a tire, rubber which undergo a large energy loss have generally been utilized in the tire's tread, for example, styrene-butadiene rubber (SBR). However, it has been very difficult to improve the wet skid resistance of a tire without sacrificing its rolling resistance.[3]

Blend rubbers and copolymers with different chain blocks are normally utilized in tire treads to balance the traction characteristics and rolling resistance. For instance, various mixtures of SBR and BR are commonly used as a rubber material for tire treads.[4,5] However, such blend rubbers can not well adjust this inconsistently viscoelasticity as assumed. Nowadays, a lot of studies have been focused on rubber materials with novel architectures, which are prepared by macromolecule design.

Tin-coupled styrene-butadiene rubbers have been reported to be a good rubber material used in tire tread,[6] because of the unique structure of the Sn-Carbon bond (Sn—C bond). In the blending process, the Sn—C bonds are firstly broken up to produce reactive centers, which may react with the functional groups on the surface of carbon black. Effect of the Sn—C bond transfer in the blending process could benefit the dispersion of carbon black so as to reduce the rolling resistance.[7,8] The coupled structure of the tin-coupled rubber also benefits to the reduction of the rolling resistance, because it contains less amount of free chain terminals.[9,10]

In our previous work, a novel multifunctional organo-lithium was used to synthesize a new kind of tin-coupled star-shaped block copolymer: tin-coupled polybutadiene-*b*-ploy(styrene-butadiene) ((SB-B)$_4$Sn). This star-shaped block copolymer contained two different types, namely *S*-PB-PSB and *S*-PB-PSB-PS, depending on the styrene content in

Correspondence to: X. Zhang (zhangxy_buct@yahoo.cn).
Contract grant sponsor: National Natural Science Foundation of China; contract grant number: 50573005.

loading solution (St%). This novel star-shaped block copolymer has a particular architecture composed of high rebound chain blocks (PB-block) and high energy loss chain blocks (PSB-block or PSB-PS-block). The PB-block was designed for reducing the rolling resistance; the PSB-block and the PSB-PS-block were designed for improving the antiskid resistance. $(SB\text{-}B)_4Sn$ was synthesized by two-stage anionic polymerization technology. The homo-polybutadiene block was formed in the first reaction stage, and the residual blocks were formed in the second stage with the presence of tetrahydrofuran (THF). *S*-PB-PSB was synthesized when the St% was lower than 34.9%, otherwise *S*-PB-PSB-PS was generated.

For exploring physical characteristics and applications of $(SB\text{-}B)_4Sn$, in this work, morphology, mechanical property, and viscoelasticity property of $(SB\text{-}B)_4Sn$ were studied and contrasted with that of the tin-coupled star-shaped random styrene-butadiene rubber (*S*-SBR) and the tin-coupled star-shaped random styrene-butadiene rubber/*cis*-1,4-structure butadiene blend rubber (*S*-SBR/*cis*-BR blend rubber), which were made in our laboratory.

EXPERIMENTAL

Materials

Cis-1,4-polybutadiene rubber (*cis*-BR), marked BR9000, was provided by Beijing Yanshan Synthetic Rubber Factory (China). Multifunctional organolithium and Star-shaped random styrene-butadiene copolymer (*S*-SBR) were made in our laboratory with the method explained elsewhere.[11,12] Carbon black N234 was purchased from Tianjin Haitun Carbon Black (Tianjin, China). Other additives were common in the rubber processing industry.

Synthesis of $(SB\text{-}B)_4Sn$

A 2-L stainless steel reactor was purged with nitrogen and subsequently washed with a living polystyryl-lithium solution. The synthesis was carried out in a two-stage procedure. The first stage was aimed to produce polybutadiene blocks (PB-blocks). Butadiene-cyclohexane solution and the multifunctional initiator were loaded into the reactor and the polymerization was performed at 50°C and 0.04 MPa pressure for 3 h. Subsequently, in the second stage, a mixture of styrene (St), 1,3-butadiene (Bd), and tetrahydrofuran (THF) in various compositions was added into the system and the polymerization continued at 50°C for another 3 h to form polystyrene or poly(butadiene-*ran*-styrene) blocks. The weight ratios of styrene to butadiene in the mixture solution were 17.9/53.8, 25.2/63.0, 36.1/48.1, 30.0/29.9, 40.6/19.8, respectively. Finally, the reaction was terminated using alcohol and 2,6-di-*tert*-butyl *para*-cresol. All reactions were conducted in nitrogen atmosphere.

TABLE I
Formulation of Different Rubber Compounds

Composition	Contents (phr)[a]
Rubber	100
Sulfur	1.8
Zinc oxide	4.0
Carbon black	50.0
Accelerator,(CZ/TT)	1.0/0.2
Stearic acid	2.0
Antiager (RD)	1.5
Liquid coumarrone	5.0

[a] phr is the abbreviation of weight parts per 100 weight parts rubber.

CZ, N-cyclohexyl-2-benzothiazole sulphenamide; TT, tetramethyl thiuram disulfide; RD, polymeried 2,2,4-trimethyl-1,2-dihydroquinoline (resin).

Preparation of vulcanizates

The samples were mixed with the additives in conventional cycles on a laboratory two-roll mill, according to the formulation given in Table I. The compounds were cured in a standard mold with about 15 MPa pressure at 150°C.

Characterization

Morphologies were tested by transmission electron microscopy (TEM, Hitachi-800-1). The specimen of $(SB\text{-}B)_4Sn$ was cast films from toluene (0.5 wt %) at room temperature and then annealed for 36 h at 130°C under vacuum. Their ultrathin samples were made by the microtome cutting of the vulcanizates frozen with liquid N_2. The specimen of *S*-SBR and *S*-SBR/*cis*-BR blends were made directly by the microtome cutting of the vulcanizates frozen with liquid N_2. All samples on copper grids were stained in OsO_4 vapor for 40 min. The TEM instrument worked at an accelerating voltage of 200 kV.

Mechanical properties of these rubbers were measured according to ASTM standards. (e.g., ASTM D2240 for shore A hardness, ASTM D412 for tensile properties, and ASTM D624 for tear strength.). For each compound, five specimens were tested, and the median of these results were reported.

Dynamic mechanical properties were measured using dynamic mechanical thermal analyzer (DMTA, DDV-11-EA, Rheometric Scientific™). These experiments were carried out in the tensile mode at a heating rate of 5°C/min, a frequency of 1 Hz, and a deformation amplitude of 0.005%. Testing

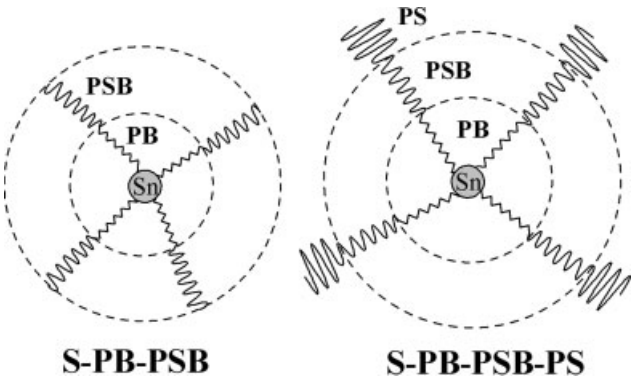

Figure 1 Sketch maps of *S*-PB-PSB and *S*-PB-PSB-PS.

temperature was varied from –120 to 100°C. The dimension of the specimens was 50 × 6 × 2 mm.

Strain sweep experiments were performed using the rubber process analyzer (RPA) of Alpha Technologies (Akron, Ohio) at a fixed frequency and 60°C. The strain was varied from 0.28 to 50% at the frequency of 1 Hz for cured vulcanizates.

Rheological properties of the samples were measured using the Instron 3211 Capillary Rheometer of Instron Company. The experiments were carried out at 100°C. The capillary length was 1.0062 in., and the capillary diameter was 0.0628 in. The piston diameter was 0.9525 cm.

RESULTS AND DISCUSSION

Microstructure analysis

Microstructure analysis methods of these star-shaped block copolymers have been reported in our previous article.[12] Architecture sketch maps of $(SB-B)_4Sn$ are shown in Figure 1, and their structure information is summarized in Table II.

In Figure 1, we can find that both of *S*-PB-PSB and *S*-PB-PSB-PS have a core-shell structure. Their core parts are formed by Sn atoms and polybutadiene blocks (PB-blocks). Shell parts are constituted by poly(butadiene-*ran*-styrene) blocks (PSB-blocks) and poly(butadiene-*ran*-styrene)-*b*-polystyrene blocks (PSB-PS-blocks), respectively.

Table II summarizes the polymer characteristics for *S*-PB-PSB, *S*-PB-PSB-PS, *S*-SBR and *S*-SBR/*cis*-BR blends. In Table II, D6 is the tin-coupled star-shaped random butadiene-styrene copolymer (*S*-SBR) with 25.5% of styrene weight percent (St%) and 36.6% of vinyl content (Bv%). Star-shaped block copolymer D2 and D3 have PB-block weight contents of 23 and 26% respectively, near to the weight content of *cis*-BR (BR9000) in *S*-SBR/*cis*-BR blend rubber D7 (25%). PB-block contents in D1, D4, and D5 are similar to the *cis*-BR content of D8 (40%). From Table II, we can also find that PB-blocks of all star-shaped block copolymers contain the similar vinyl content ranged from 18 to 21%, whereas the vinyl content of *cis*-BR in the *S*-SBR/*cis*-BR blend rubber is about zero. In contrast, *S*-SBR and the *S*-SBR parts of *S*-SBR/*cis*-BR blend rubbers have larger vinyl content than the PSB-block in *S*-PB-PSB and *S*-PB-PSB-PS. In addition, all of the samples have wide molecule weight distributions around 1.8, which implies they possess good processing properties.

Morphology analysis

In Figures 2–4, TEM micrographs of *S*-PB-PSB, *S*-PB-PSB-PS, *S*-SBR and *S*-SBR/*cis*-BR blend rubbers are shown.

In sample D1 and D2, there are two types of blocks: homogenous PB-blocks and butadiene-*ran*-styrene ones (PSB-blocks). It is indicated in Table II that PSB-blocks possess low styrene content (25.0 wt % and 28.6 wt %), and thus they are compatible with homo-PB ones. As a result, their morphologies exhibit a continuous single-phase (Fig. 2).

In sample D3, homo-PS blocks are formed. Because the PSB-blocks possess a higher styrene content, it becomes compatible with homo-PS blocks and incompatible with homo-PB blocks. As a result of phase separation (Fig. 3), homo-PB blocks form islands dispersed in a sea of PSB-blocks and homo-PS blocks.

TABLE II
Microstructures of Different Vulcanizates

Properties	S-PB-PSB		S-PB-PSB-PS			S-SBR	S-SBR/cis-BR	
	D1	D2	D3	D4	D5	D6	D7	D8
PB/PSB/PS (wt %)	40/60/0	23/77/0	26/70/4	41/52/7	48/36/16	—	—	—
BR9000/S-SBR	—	—	—	—	—	0/100	25/75	40/60
Bv/PB (wt %)	18.3	18.0	19.2	20.0	20.4	—	0	0
St/PSB (wt %)	25.0	28.6	39.4	43.4	52.9	25.5	25.5	25.5
Bv/PSB (wt %)	26.3	21.1	15.9	11.1	5.1	36.6	36.6	36.6
Mn (kg/mol)	169	340	170	196	120	350	—	—
Mw/Mn	1.7	1.8	1.5	1.9	1.8	1.8	—	—

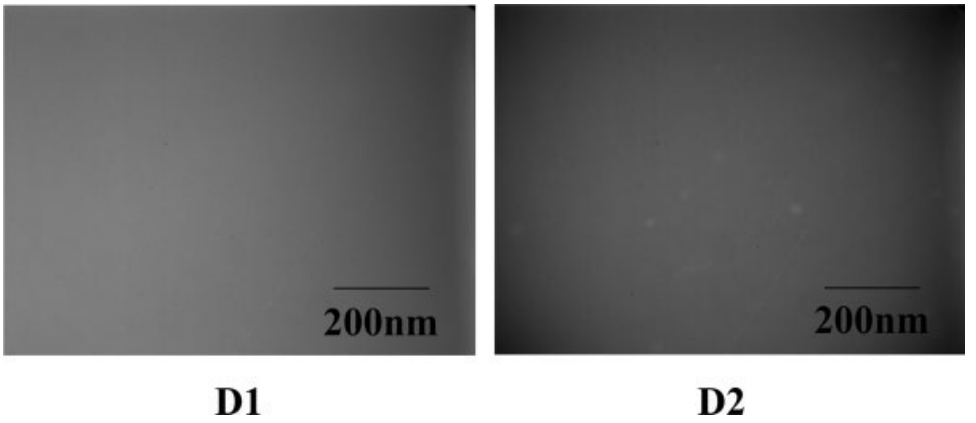

Figure 2 TEM images of *S*-PB-PSB (stained with OsO_4 for 40 min).

Sample D4 contains the same type of blocks as D3, but its TEM picture shows structures that are not well defined. This is caused by the increasing of styrene content and PB-block content. On one side, increment of the styrene content further decreases the compatibility between PB-blocks and PSB-PS-blocks; on the other side, the large PB-blocks content causes more tangle points among PB-block chains. As a result, interface between PB-blocks and PSB-PS-blocks became distinct.

As shown in TEM picture of D5 (Fig. 3), further increment of styrene content leads to a laminar, two-phase morphology.

In Figure 4, D6 shows a homogenous, continuous single-phase. This indicates that the styrene units are totally random distributed in *S*-SBR.

In sample D7, the weight ratio of *S*-SBR to *cis*-BR is 75/25. TEM picture shows that the gray *S*-SBR domains are separated by black *cis*-BR domains. However, the interfacial layers between black domain and gray domain are not obvious, and the *cis*-BR domain is mingled with gray area.

With the *cis*-BR content increases to 40 wt %, two separated phases can be found in TEM picture of D8. The black one is the *cis*-BR phase, and the gray one is the *S*-SBR phase. Their distinct interfacial layers illustrate the dispersion of *cis*-BR became worse in *S*-SBR/*cis*-BR compound.

In summary, it can be found from TEM pictures (Figs. 2–4) that the PB-blocks can be uniformly distributed in the star-shaped block copolymers. On the contrary, *cis*-BR has a poor dispersion in the *S*-SBR/*cis*-BR blend rubbers. Moreover, with the increasing of *cis*-BR content, the dispersion becomes worse.

Mechanical property analysis

Mechanical properties of the samples are listed in Table III.

From Table III, we can find that modulus at 300% elongation (300% modulus) of star-shaped block copolymers near to 12 MPa, and is slightly lower than that of star-shaped random copolymer *S*-SBR and *S*-SBR/*cis*-BR blend rubbers. In the star-shaped block copolymer chains, PB-blocks and PSB-blocks (or PSB-PS-blocks) join into the molecule chains in tandem by Carbon—Carbon bond connection. When the rubbers receive the stretch, the rigid shell parts (PSB-blocks or PSB-PS-blocks) can rapidly transmit the stress to the soft PB-blocks, which have lower modulus and then will undergo larger deformation under low stress. In addition, high styrene content in PSB-blocks (or PSB-PS-blocks) leads to a low crosslink density, which will also decrease their 300% modulus. In contrast, for *S*-SBR/*cis*-BR blend rubbers (D7 and D8), *S*-SBR chains and *cis*-BR chains

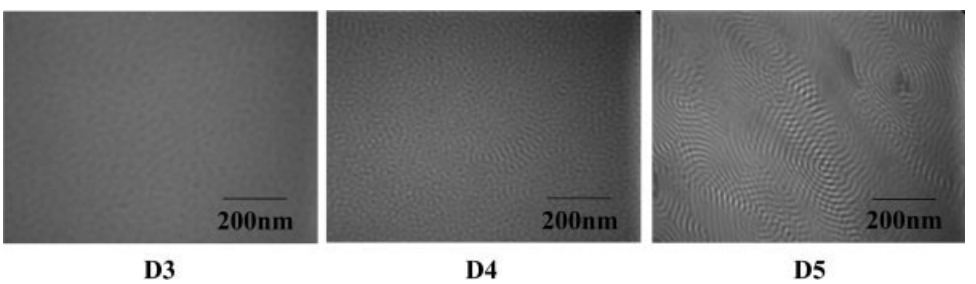

Figure 3 TEM images of *S*-PB-PSB-PS (stained with OsO_4 for 40 min).

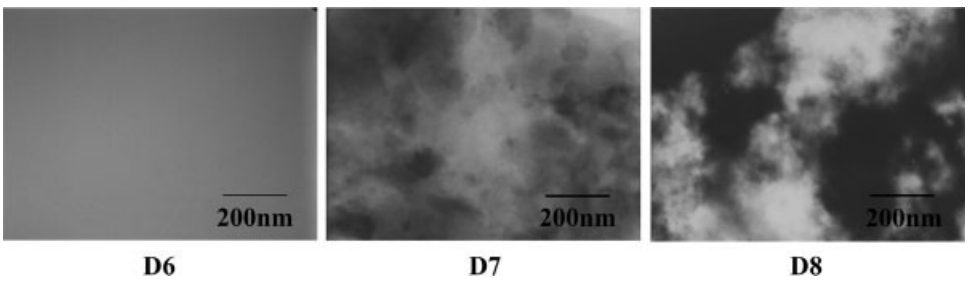

Figure 4 TEM images of *S*-SBR and *S*-SBR/*cis*-BR blend rubber (stained with OsO_4 for 40 min).

aren't connected in the same way, resulting in different stress transfer pattern. When the blend rubber is stretched, the stress is mainly withstanded by *S*-SBR chains, which is rigid and hard to be deformed. Therefore, the star-shaped block copolymers have smaller 300% modulus than *S*-SBR and *S*-SBR/*cis*-BR.

Tensile strength of D2 and D3 are 17.6 and 20.2 MPa respectively, near to that of *S*-SBR/*cis*-BR compound D7 (18.9 MPa), because they have the similar polybutadiene content. D4 and D5 also have the similar polybutadiene content with D8, but their tensile strengths are higher than that of D8. This may be caused by the reinforcing effect of the PS-blocks in the star-shaped block copolymer chain ends. Compared with star-shaped random copolymer *S*-SBR, star-shaped block copolymers have a slightly lower tensile strength because of the existence of PB-blocks.

Table III shows that the star-shaped block copolymer without PS-blocks (D1 and D2) has a smaller value of elongation at break (<400%), as well as the *S*-SBR/*cis*-BR blend rubber (D7 and D8). On the contrary, the star-shaped block copolymer with a few PS-blocks (≤7%), for example D3 and D4, displays higher value of elongation at break (>400%).

Styrene units in PS-block segments have bigger influence on hardness than styrene units distributed randomly. From Table III, we can find that styrene contents of D1, D2, and D6 are 15.0, 22.0, and 25.5% respectively, whereas their hardness varied slightly. When the PS-block formed in the copolymers, hardness increased sharply with the rise of the PS-block content. In Table III, PS-block contents of D3, D4, and D5 are 4, 7, and 16% respectively; correspondingly their hardness is 74, 75, and 88. For *S*-SBR/*cis*-BR blend rubbers, *cis*-BR content has little effect on the hardness property. In addition, abrasion loss value of all samples is closely related to rubbers hardness. The higher hardness value leads to a lower abrasion loss value.

Table III shows that permanent set of star-shaped block copolymer is obviously affected by styrene content. In contrary, effect of PB-block is slight. In architecture of star-shaped block copolymers, PB-blocks and PSB-blocks (or PSB-PS-blocks) connect in series. With the increase of styrene content, the rigidity and plasticity of molecular chains in the shell parts enhance, but the flexible segment and the elasticity reduce simultaneously. When the deformation occurs, the rigid chain segment can hardly recover their deformation; therefore, the permanent set is bigger. In the blend rubber, influence of *cis*-BR content on permanent set is obvious. With the *cis*-BR content increases from 0 to 40%, permanent set decreases from 11% to 7%.

As is shown in Table III, star-shaped block copolymers have the similar tear strength value with *S*-SBR and *S*-SBR/*cis*-BR compounds. Increase of styrene content has little effect on the tear strength. Cis-BR content also has little effect on the tear strength of blend rubbers (D7 and D8).

Dynamic mechanical thermal analyzer analysis

It is the aim of high performance tire treads to possess the combination properties of good antiskid

TABLE III
Mechanical Properties of Different Vulcanizates

	S-PB-PSB		S-PB-PSB-PS					
	D1	D2	D3	D4	D5	D6	D7	D8
Modulus at 300% elongation (MPa)	11.7	13.7	12.2	11.6	15.6	15.0	16.1	13.3
Tensile strength (MPa)	15.7	17.6	20.2	20.4	19.4	22.0	18.9	17.4
Elongation at break (%)	390	376	445	462	383	406	356	373
Shore a hardness	69	71	74	75	88	71	72	71
Permanent set (%)	12	10	16	16	20	11	6	7
Tear strength (KN/M)	40.3	46.2	41.4	47.3	48.8	47.0	47.4	45.9
Abrasion loss (cm^{-3}/1.61 km)	0.305	0.235	0.143	0.100	0.091	—	—	—

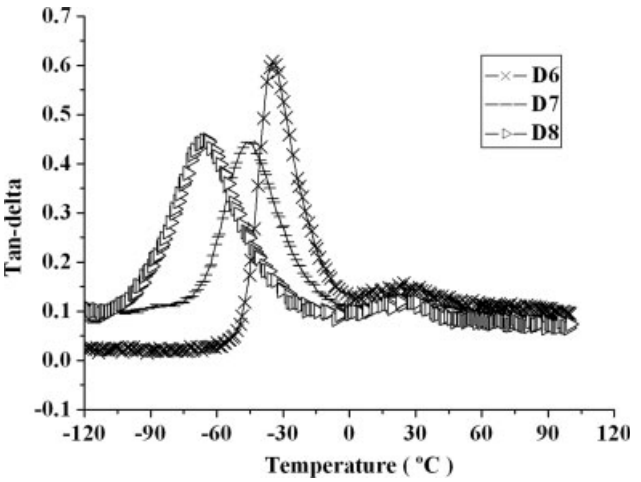

Figure 5 DMTA spectra (tan-delta) of *S*-SBR and *S*-SBR/*cis*-BR blend rubber.

properties under wet conditions and low rolling resistance. Saito[2] found that rubber having high tan delta value at 0°C shows good wet traction property, and the rubber possessing low tan delta value at 60°C exhibits low rolling resistance. So the ideal rubber needs to show the combination of high tan delta value at 0°C and low tan delta value at 60°C.[13] In addition, it was reported that tan delta value at −25°C can indicate the antiskid properties on snow and ice road surface.[10] The higher value of tan delta at −25°C, the better antiskid properties rubber will have.

Dynamic viscoelasticity analysis

Figure 5 shows the DMTA spectrums of *S*-SBR (D6) and *S*-SBR/*cis*-BR blend rubbers (D7 and D8). *S*-SBR has a narrow loss peak ranging from –50°C to –6°C. The maximum value of tan delta is 0.61, appearing at –35°C. With the increasing of *cis*-BR content, loss peak of *S*-SBR/*cis*-BR compound shifts from high temperature area to low temperature area and becomes broader. The maximum tan delta value of D7 is 0.44, appearing at –45°C; the maximum tan delta value of D8 is 0.45, appearing at –64°C. In Figure 5, it is interesting to note that D6, D7, and D8 approach the same tan delta value (about 0.1) when temperature is above 0°C.

According to the structure-property relationship of styrene-butadiene copolymer, the order of structures enlarging the rolling resistance and antiskid properties is "free terminals" > styrene group > vinyl group.[14–16] The "free terminals" can motion freely and lead to large hysteresis, which is the key factor contributing to poor rolling resistance and heat accumulation. On the contrary, the vinyl group has little effect on rolling resistance whereas obvious effect on wet grip performance. Thus, fall of wet grip performance because of decreasing free terminals concentration could be offset so much as enhanced by increasing vinyl content. *S*-SBR initiated by tin-coupled multifunctional initiator has less "free terminals" content than linear copolymers. Thus *S*-SBR shows lower rolling resistance and smaller tan delta at 60°C (0.11). On the other side, this tin-coupled structure also make *S*-SBR to have lower tan delta at 0°C (0.13), which indicates that the antiskid property of *S*-SBR needs to be enhanced. PSB-blocks and PSB-PS-blocks in star-shaped block copolymers have higher styrene content than *S*-SBR. The styrene units can enhance the antiskid property because of their higher internal friction resistance during the molecular chain movement. PB-blocks in star-shaped block copolymers have been designed for improving the antiskid property on ice and snow surface. Tan delta curves of star-shaped block copolymers are shown in Figure 6.

In Figure 6, D1, D2, and D3 show single loss peak, and their maximum tan delta value are 0.57, 0.52, and 0.40, respectively. With the increasing of styrene content within PSB blocks and PSB-PS blocks, their loss peaks move from lower temperature area to 0°C. Styrene content (St%) of D1 is 25.0%, and the loss peak appears at –30°C. St% of D2 is 28.6%, and the loss peak at –20°C. St% of D3 is 39.4%, and the loss peak at –3.5°C. D4 possesses a special wide loss peak ranging from –60 to 30°C. The maximum tan delta value is 0.27 at –6°C. DMTA spectrum of D5 shows two loss peaks far apart from each other, which is caused by the reason that the incompatibility between PB-blocks and PSB-PS-blocks induces strong phase separation (seen in Fig. 3). The low peak at −66°C for PB-blocks and the one at 47°C for the composed phase of PSB-blocks and PS-blocks.

Tan delta data of these samples at different temperatures are listed in Table IV.

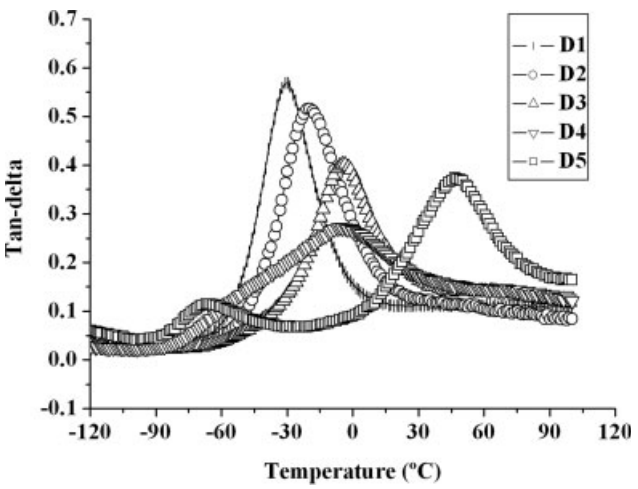

Figure 6 DMTA (tan-delta) spectra of star-shaped block copolymers.

TABLE IV
Tan Delta Value of Different Vulcanizates at −25, 0, and 60°C

	S-PB-PSB		S-PB-PSB-PS					
Tan δ	D1	D2	D3	D4	D5	D6	D7	D8
−25 °C	0.51	0.46	0.17	0.22	0.05	0.42	0.22	0.12
0 °C	0.16	0.28	0.38	0.27	0.09	0.13	0.11	0.10
60 °C	0.11	0.10	0.14	0.15	0.30	0.11	0.10	0.08

In Table IV, D1, D2, D6, D7, and D8 show smaller tan delta value than the others at 60°C. It implies better low rolling resistance. D1, D2 have the similar tan delta value with D6 because of their tin-coupled architecture and low "free terminals" content. In *S*-SBR and *S*-SBR/*cis*-BR blended rubber D7 and D8, with the *cis*-BR content increase from 0 to 40%, the tan delta value at 60°C decrease from 0.11 to 0.08. This result shows that *cis*-BR component in blend rubbers can reduce the tan delta value of *S*-SBR/*cis*-BR compound. The *cis*-BR component shows better chain flexibility and lower internal friction with *S*-SBR chains, so it is helpful for reducing the rolling resistance. Table IV shows that tan delta of D3 and D4 is 0.14 and 0.15 respectively, a little higher than that of *S*-SBR, because PS-blocks in their chain ends may cause larger internal friction resistance at 60°C.

From Table IV, we could find that the star-shaped block copolymer have bigger tan delta value than *S*-SBR at 0°C, and the *S*-SBR/*cis*-BR blend rubbers has the smallest tan delta value. *S*-SBR with low styrene content (25.5%) has a narrow loss peak ranging from −50°C to –6°C. Their chain segments have already finished their transformation from glass state to rubbery state when the temperature reaches –6°C from lower temperature. Then the internal friction begins to decrease with the raise of temperature. As a result, the tan delta of *S*-SBR at 0°C fell down to a smaller value. For star-shaped block copolymers, on one side, PB-blocks make the loss peaks have the tendency to move from high temperature area to low temperature area; on the other side, large styrene content in PSB-blocks and PSB-PS-blocks make their loss peaks shift to the opposite orientation. As a result, their loss peaks are closed to 0°C, and their tan delta values at 0°C near to the maximum value. So we could conclude that D1, D2, D3, and D4 have better antiskid properties than *S*-SBR under wet conditions. Although blend rubber D7 and D8 have the large number of free terminals, their styrene content and vinyl content are too low to provide enough wet grip resistance.

In addition, D1 has a tan delta value of 0.51 at –25°C, and that of D2 is 0.46, as big as that of *S*-SBR (0.43). All of these tan delta values are further higher than that of blend rubber *S*-SBR/*cis*-BR (0.22 and 0.12). Thus D1, D2 might have outstanding antiskid properties on snow and ice surface, similar to *S*-SBR.

Through contrasting the tan delta values of all samples at different temperatures, we could find that D2 has the best overall dynamic mechanical properties. D3 and D4 have better antiskid properties under wet conditions than *S*-SBR and *S*-SBR/*cis*-BR blend rubbers. D1 has low rolling resistance and outstanding antiskid properties on snow and ice surface like *S*-SBR. Moreover, its antiskid property on wet conditions is better than that of *S*-SBR and blend rubber *S*-SBR/*cis*-BR. Copolymer D5 contains too many PS-blocks, which lead to a high rolling resistance, thus it is not suitable to be used in tire tread.

According to our previous research, *S*-SBR has been confirmed to have good overall mechanical properties required by high performance tire tread. Star-shaped block copolymer *S*-PB-PSB and *S*-PB-PSB-PS not only have the similar mechanical properties with *S*-SBR, but also possess the good combination of low rolling resistance and outstanding antiskid properties both on snow surface and on wet conditions. So we could conclude that *S*-PB-PSB and *S*-PB-PSB-PS have satisfied the requirements of high performance tire tread.

Storage modulus analysis

Figure 7 shows storage modulus as function of temperature for different samples. At the beginning, the storage moduli of all the samples decrease sharply with the rise of temperature. When temperature increases over 60°C, the storage moduli decrease slightly.

Storage moduli of star-shaped block copolymers in the glass state are higher than that of *S*-SBR and the *S*-SBR/*cis*-BR blend rubbers because the

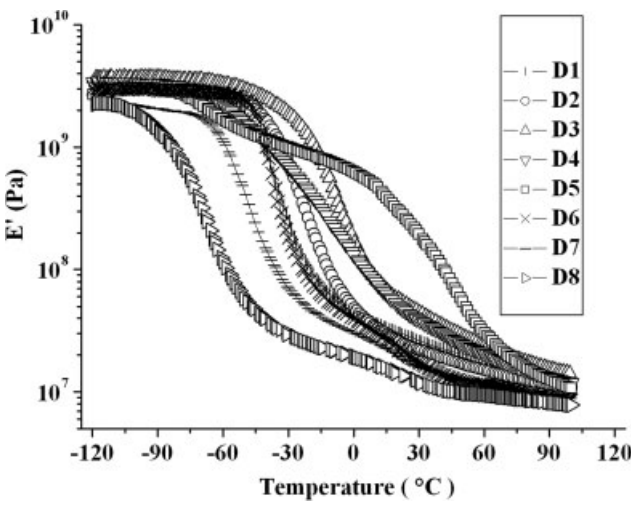

Figure 7 Modulus-temperature relationships of different rubbers.

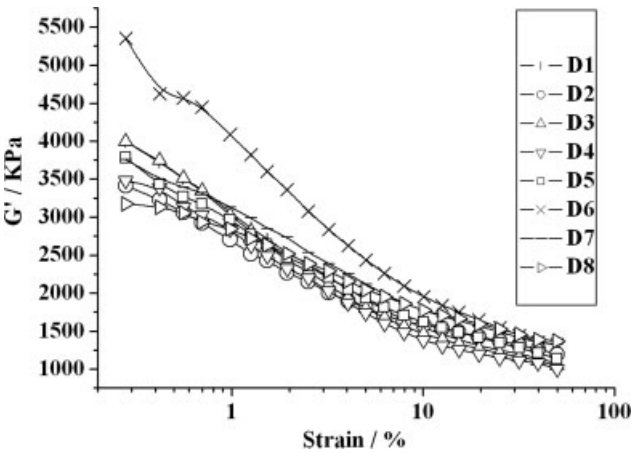

Figure 8 RPA analysis (storage moduli) of different vulcanizates.

molecular chains of star-block copolymers with the block architectures and tin-coupled structures pile up closely together and the free volume among the chains is smaller. In addition, high styrene content in PSB-blocks (or PSB-PS-blocks) and the fixed structure of PB-blocks make the deformation of star block copolymers only happen under strong stress. Although *S*-SBR also has a coupled structure, the random array distribution of the styrene units makes the molecular chains stack in a looser structure and the free volume is larger. As a result, storage modulus of *S*-SBR is smaller. In *S*-SBR/*cis*-BR compound, *cis*-BR components disperse nonuniformly in *S*-SBR matrix, and a lot of free volumes exist among the interfaces between *cis*-BR phases and *S*-SBR phases. The interaction force of the boundary between *cis*-BR and *S*-SBR is weak, and the molecular chains can move easily, so the storage modulus of *S*-SBR/*cis*-BR blend is also smaller.

In the glass-transition zone, the order of storage moduli is *S*-PB-PSB-PS > *S*-PB-PSB > *S*-SBR > *S*-SBR/*cis*-BR blend rubber. Molecular chain ends of star-shaped copolymers are fixed by the $SnCl_4$ coupler, so the relaxation of molecular chains becomes difficult. PS-blocks in the chain ends of *S*-PB-PSB-PS enhance the entanglement effect of the molecular chain, so the relaxation becomes more difficult. As a result, storage modulus of *S*-PB-PSB-PS is the largest in all samples (seen as D3, D4, and D5).

Rubber processing analyzer analysis

Dynamic viscoelastic properties of the samples were performed by RPA2000, which can carry out strain and frequency scanning in a board range. The spectra of the RPA2000 can reflect the information of the dispersion of additives in rubber matrix.[17] The dependency of the storage modulus (G′) of the cured samples on the strain amplitude is shown in Figure 8. The modulus decreases dramatically when the strain amplitude is less than 10%. It can be explained by two reasons: one is the breakdown of filler-rubber networks constructed by filler-filler interaction and filler-rubber interaction; the other is that large carbon agglomerates may break into small aggregates under the deformation of rubbers. Then, when the strain amplitude is larger than 10% modulus curves decrease smoothly, because small aggregates are hardly to be crumbled under this testing condition.

It is easily to find in Figure 8 that D6 has the largest discrepancy between the maximum G′ and the minimum G′, and *S*-SBR/*cis*-BR blend rubber (D7 and D8) has the smallest one. According to the Payne effect, smaller discrepancy implies better filler-rubber interaction, and better dispersion of additives in rubber matrix.[18–20] Thus, D7 and D8 have good filler-rubber interactions, and additives disperse well in *S*-SBR/*cis*-BR compound rubber matrix. *S*-SBR has the worst dispersion of additives among all samples. We could find that the *cis*-BR component in *S*-SBR/*cis*-BR blend rubber has positive effect on the filler-rubber interaction and the dispersion of additives.

The star-shaped block copolymer *S*-PB-PSB and *S*-PB-PSB-PS have similar G′ discrepancy with D7 and D8, and the additives are also dispersed well. This result implies that PB-blocks in block copolymers can also benefit the dispersion of additives. In addition, the fact that the dispersion of additives in D4 is better than in D3 illustrates that more PB-block content may lead to better dispersion of additives. The same conclusion can be drawn on the *cis*-BR component in blend rubbers.

Figure 9 shows the relationship between tan delta value and the strain amplitude at 60°C. The tan delta value curves rise at the lower strain amplitude area, then decrease in the middle, and rise again at the higher strain amplitude area. Tan delta value of

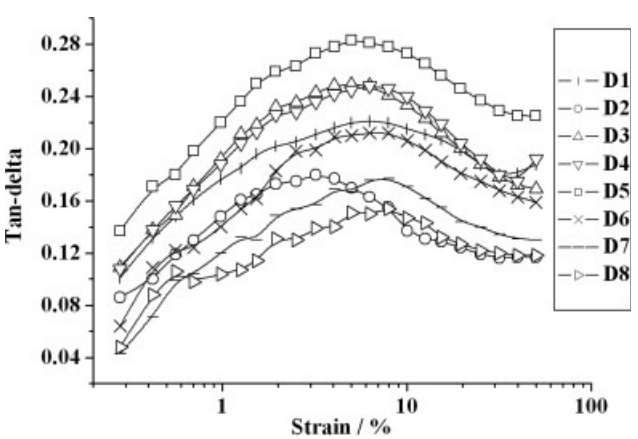

Figure 9 RPA analysis (tan delta value) of different vulcanizates.

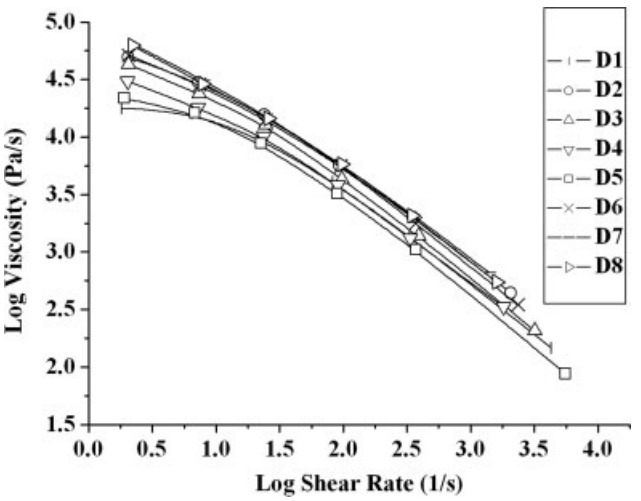

Figure 10 Rheological property of different uncured rubber compounds.

all samples reaches to the maximum value in the strain amplitude zone ranging from 3 to 10%. Higher tan delta value implies higher friction between additives and rubber chains. When the strain amplitude reaches to 40%, tan delta value gets to a minimum value. This may have caused by the breakdown of filler-rubber network which becomes weak in the large strain amplitude. The raise of tan delta value at the end may cause the slippage of the whole molecule chain and partially rupture of the crosslink net work of rubber matrix.

Cis-BR has lower filler-rubber friction and dynamic heat build up than other rubbers because its *cis*-1,4-structure content near to 100% and the molecular chain segments are quite flexible. So *S*-SBR/*cis*-BR blend rubber (D7 and D8) shows lower tan delta value than the others at the same strain amplitude.

PB-blocks in star-shaped block copolymers have low vinyl content and good molecular chain flexibility, so they can also display smaller internal friction between additives and rubber matrix. The difference between PB-blocks and *cis*-BR components is that one side of the PB-block is coupled by $SnCl_4$ coupler, and the other chain side is connected with the PSB-block (or the PSB-PS-block) by Carbon—Carbon bonds. So the thermal vibration of the PB-block segments is restricted. Figure 9 shows that D2 has a similar tan delta value with D7 and D8. It implies that PB-blocks have the similar effect on decreasing the friction between rubber matrix and fillers.

PS-blocks in star-shaped block copolymers may cause increment of the internal friction because of their large number of phenyl structures. D3 and D4 show slightly higher tan delta value than *S*-SBR in Figure 9, and it can be attributed to their PS-blocks.

Rheological analysis

Apparent viscosity as functions of shear rate for the uncured carbon black compounds is displayed in Figure 10. Figure 10 shows that these samples have characteristic of non-Newtonian pseudoplastic fluid. At the same shear rate, the order of viscosity of uncured carbon black compounds is *S*-SBR/*cis*-BR compounds > *S*-SBR > D2 > D3 >D4 and D1 > D5. We could find that *S*-PB-PSB-PS and *S*-PB-PSB have lower viscosity, which implies that they may have better processing properties than rubber compounds.

CONCLUSIONS

Tin-coupled star block copolymer $(SB\text{-}B)_4Sn$, which contained two different types: *S*-PB-PSB and *S*-PB-PSB-PS was produced via two-stage continuous living anionic polymerization with a multifunctional initiator. This new star block copolymer with both high rebound chain blocks (like PB blocks) and high energy loss chain blocks (like PSB and PSB-PS blocks) shows various morphologies. The *S*-PB-PSB display homogenous morphology. The *S*-PB-PSB-PS display separated morphology. Mechanical testing results show that *S*-PB-PSB and *S*-PB-PSB-PS possess similar mechanical properties with *S*-SBR and *S*-SBR/*cis*-BR blend rubber. DMTA results display that tan delta values of *S*-PB-PSB and *S*-PB-PSB-PS (PS $\leq$ 7%) are higher than that of *S*-SBR and *S*-SBR/*cis*-BR blend rubber at –25°C and 0°C, respectively. At 60°C, PS-PB-PSB and *S*-PB-PSB-PS have the same tan delta value with *S*-SBR and *S*-SBR/*cis*-BR compound. Thus *S*-PB-PSB and *S*-PB-PSB-PS (PS $\leq$ 7%) display good combination of low rolling resistance and high antiskid resistance on both snow surface and wet road conditions. RPA testing result shows that PB-blocks in star-shaped block copolymers may give rise to better dispersion of additives, so close the *cis*-BR component of *S*-SBR/*cis*-BR blend rubber. Rheological property illustrates that *S*-PB-PSB and *S*-PB-PSB-PS have better processing properties than *S*-SBR and *S*-SBR/*cis*-BR blend rubber. Overall, these tin-coupled star-shaped block copolymers show good mechanical and dynamic characteristics, and could be considered for application in high performance tire tread.

References

1. Hsu, W. L.; Halasa, A. F.; Matrana, B. A. U.S. Pat. 5,541,264 (1996).
2. Saito, K.Y. Kautschuk Gummi Kunststoffe 1986, 39, 30.
3. Chen, S. C. China Synth Rubber Ind 1997, 20, 6.
4. Hsu, W. L.; Halasa, A. F.; Matrana, B. A. U.S. Pat. 5,422,403 (1995).
5. Halasa, A. F.; Hsu, W. L.; Zanzig, D. J. U.S. Pat. 5,534,592 (1996).

6. Tsutsumi, F.; Sakakibara, M.; Oshima, N. Rubber Chem Technol 1990, 63, 8.
7. Zhao, S. H.; Wang, Z. China Synth Rubber Ind 2000, 23, 20.
8. Zhao, S. H.; Zhang, X. Y.; Jin, G. T. J Appl Polym Sci 2003, 89, 2311.
9. Lu, J. M.; Zhang, X. Y.; Zhao, S. H. J Appl Polym Sci 2007, 104, 3917.
10. Lu, J. M.; Zhang, X. Y.; Zhao, S. H. J Appl Polym Sci 2007, 104, 3924.
11. Zhang, X. Y.; Jin, G. T.; Zhao, S. H. U.S. Pat. 6,150,487 (2000).
12. Feng, H. D.; Zhang, X. Y.; Zhao, S. H. J. Appl Polym Sci 2008, 110, 228.
13. Nordsiek, K. H. Kautschuk Gummi Kunststoffe 1985, 38, 178.
14. Takao, H.; Imai, A. China Synth Rubber Ind 1987, 1 (Suppl.), 33.
15. Kern, W. J. Futamura, S. Polymer 1988, 29, 1801.
16. Wilder, C. R.; Haws, J. R. Kautschuk Gummi Kunststoffe 1984, 37, 683.
17. Jia, Q. X.; Wu, Y. P.; Wang, Y. Q. J Appl Polym Sci 2007, 103, 1826.
18. Payne, A. R. In Reinforcement of Elastomers; Kraus, G., Ed; Wiley: New York, 1965, Chapter 3, pp 69.
19. Karasek, L.; Meissner, B.; Asai, S. Polymer J 1996, 28, 121.
20. Kluppel, M.; Schuster, R. H. Rubber Chem Technol 1997, 70, 243.